Yb^{3+} doping in 2D $(C_8H_9NH_3)_2PbBr_4$ nanoplatelets and its optical properties

A Thesis

Submitted to

Indian Institute of Science Education and Research (IISER), Pune

In partial fulfilment of the requirements of the

BS-MS Dual Degree Programme

By

Athunya P

Reg. No: 20151020

Under the supervision of

Dr. Angshuman Nag

Associate professor, Department of Chemistry

Indian Institute of Science Education and Research(IISER), Pune

Dr. Homi Bhabha Road, Pashan, Pune 411008, INDIA.

March 2020

Certificate

This is to certify that this dissertation entitled **"Yb^{3+} doping in 2D $(C_8H_9NH_3)_2PbBr_4$ nanoplatelets and its optical properties"** towards the partial fulfilment of the BSMS dual degree programme at the Indian Institute of Science Education and Research, Pune represents study/work carried out by **Athunya P** at IISER Pune under the supervision of **Dr. Angshuman Nag**, Associate professor, Department of Chemistry, IISER Pune during the academic year 2019-2020.

Date: 20th March, 2020
Place: Pune (Maharashtra)

Athunya. P
5th year BSMS student
IISER Pune

Dr. Angshuman Nag
Associate Professor
Department of Chemistry
IISER Pune
29/03/2020

Declaration

I hereby declare that the matter embodied in the report entitled **"Yb^{3+} doping in 2D $(C_8H_9NH_3)_2PbBr_4$ nanoplatelets and its optical properties"** are the results of the work carried out by me at the Department of Chemistry, IISER Pune, under the supervision of **Dr. Angshuman Nag** and the same has not been submitted elsewhere for any other degree.

Date: 20th March, 2020
Place: Pune (Maharashtra)

Athunya. P
5th year BSMS student
IISER Pune

Dr. Angshuman Nag
Associate Professor
Department of Chemistry
IISER Pune
29/03/2020

Acknowledgements:

First of all, I would like to express my sincere thanks and gratitude to my thesis supervisor, **Dr. Angshuman Nag** .Throughout this thesis, as everyone who does this, I came across difficulties, lack of knowledge, technical difficulties, emotional stress, and a few other things. And Dr. Angshuman Nag helped me throughout giving guidance and direction, clearing my doubts, helping me solve experimental errors, giving suggestions related to my experiments, immense support and encouragement while doing the experiments, no matter what I came across, I knew I could count on my supervisor to guide me through it. His dedication to the research and his enthusiasm kept me constantly engaged on my work and motivated me to show interest in research area throughout my thesis.

I'd like to express my gratitude to **Dr. Pramod Pillai** for helping me to see the shortcomings of my thesis during mid-year presentation and help me to see new ways to improve it by discussing it further. His guidance helped me to see what I needed to accomplish my thesis results.

I'm very thankful to my institute IISER Pune and its director **Prof. Jayant B. Udgaonkar** for giving me an opportunity to do my research work

To my incredibly patient and persistently helpful and supportive lab members; Anuraj, Vikas, Tariq, Arfin, Parikshit, Rayan, Barnali, Sajid, Taniya, and my friends as well as batchmates- Vaibhav, Shivam, and Mayank, if it wasn't for you guys, even with the support of everyone else, I wouldn't have made it through thesis who gave me suggestions emotional support and made me do the experiments enjoyable. I would like to express my sincere gratitude to Tariq, whenever I encountered difficulties or needed assistance with evaluating data I had, as an experienced senior, he'd my first choice to ask for it. He always helped me for that and made suggestions to improve my work.

My sincere gratitude to Achan, amma and grandma; the pillars of my life for their love, care and affection. I am grateful to have friends in particular, Haritha, Aswani, Kiran, Nupur, etc. who made my IISER life special. A special thanks to my friend who were with me in all my ups and downs with constant support from afar.

I would like to thank SAIF-IIT Bombay for ICP-AES analysis, AFM operator Mahesh Jadhav, TEM Operator and FESEM operators. Also, Dr, Pramod Pillai's lab for DRS measurements. And I acknowledge IISER Pune for the INSPIRE fellowship.

Table of Contents

List of figures

List of table

Abstract: Lead halide perovskites are the class of materials which has wider applications in optoelectronic devices like light emitting diodes (LEDs), high efficient solar cells, and lasers. They exhibit tunable band gap which covers entire visible range, solution processability, defect tolerance, narrow and intense photoluminescence. Doping metal ions into the lattice of 3D lead halide perovskites has been used as strategy to introduce new optical functionalities, and also to improve the structural stability of the host. Transition metal ions such as Bi^{3+}, Mn^{2+} were successfully doped by substitution of Pb^{2+} in lead halide perovskite lattices. Recently 2D layered hybrid perovskites have also been reported to show interesting optoelectronic properties. In difference to 3D perovskites, these 2D perovskites show high excitonic binding energy of the order of 300-400 meV, along with superior moisture stability. Mn-doping is also reported in 2D perovskites showing intense yellow emission from transitions involving Mn d-electrons. However, we are not aware of lanthanide doping in these 2D hybrid perovskites. In this thesis, we doped Yb^{3+} in colloidal $(C_8H_9NH_3)_2PbBr_4$ nanoplatelets to obtain near infrared (NIR) emission of Yb^{3+} f-electrons. $(C_8H_9NH_3)_2PbBr_4$ is a 2D perovskite showing intense excitonic emission in the visible region, and hence a good host for doping. Our colloidal $(C_8H_9NH_3)_2PbBr_4$ nanoplatelets show high photoluminescence quantum yield for excitonic emission at 415 nm. After Yb^{3+} doping, the Yb^{3+} doped $(C_8H_9NH_3)_2PbBr_4$ nanoplatelets show NIR emission at 998 nm. Mechanistic studies suggest that the host absorb light and then non-radiatively transfers the excitation energy to the Yb^{3+} dopants. Subsequently, the Yb^{3+} ions de-excite emitting NIR lights. Further study in this direction may lead to applications in NIR LEDs and remote sensing.

1. Introduction: Three dimensional metal halide perovskite are the class of materials with general formula ABX_3 in which monovalent cations like cesium (Cs^+), methylammonium (MA^+) or formamidinium (FA^+) fit in the A site whereas divalent cations like Pb^{2+}, Sn^{2+} fit in the B site, X represents the halide site in which Cl^-, Br^-, I^- fit in it.[1] This 3D metal halide perovskites consist of corner shared network of lead-halide octahedra and these octahedra are connected in all the three directions. As a result of this 3D network, cuboctahedral voids are created. Cations like Cs^+, FA^+ or MA^+ fit into such void.[1, 20] The size of the void is fixed. When larger organic cations are introduced which can't fit into this void, these 3D networks will break and separate in to layers. This give rise to 2D network of lead halide octahedra. In third direction there is no direct contact/chemical bond.[1]

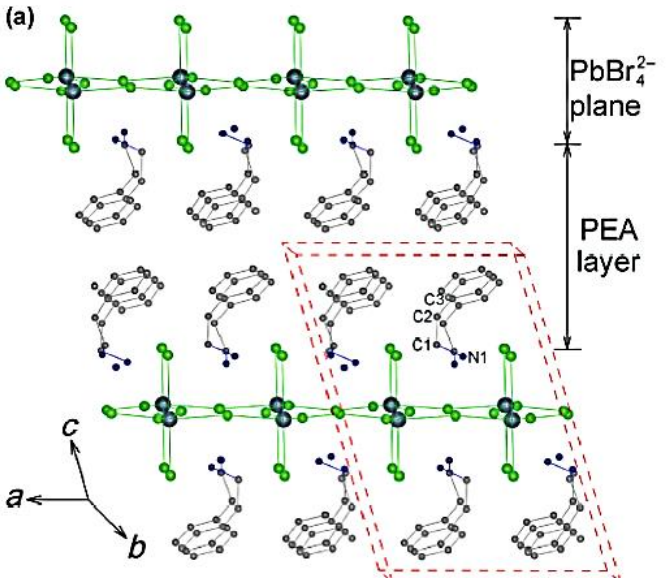

Figure 1: Extended crystal structures of $(PEA)_2PbBr_4$ along the b axis where PEA is $C_8H_9NH_3^+$. In PEA, nitrogen, carbon corresponds to smaller blue and grey spheres. In $PbBr_4^{2-}$ plane, bromine, lead represents the green and big blue spheres. Taken from ref.1 with permission, copyright 2017, Springer nature

The 2D perovskite layers are held together by weak Vander Waals forces. The semiconducting inorganic layers are separated by insulating organic layers. So this 2D

lead halide perovskite consist of extended 2D network of lead halide corner shared octahedra and two layers of organic cation capping from both the sides of inorganic lead halide octahedra to balance the charge; as can be clearly seen from the figure 1. Figure 1 represents the 2D arrangement of $(C_8H_9NH_3)_2PbBr_4$ (phenyl ethyl ammonium lead bromide) which is a 2D perovskite. The amine groups of phenyl ethyl amine (PEA) in the $(C_8H_9NH_3)_2PbBr_4$ perovskites create a hydrogen bond with $[PbBr_4]^{2-}$ framework.[1, 5 ,12] Here the structure clearly indicates that it's a layered kind of structure as the third dimension is broken. Semiconducting inorganic layers have lower band gap compared to the HOMO-LUMO gap in insulating organic cations. Hence repetition of semiconducting as well as insulating layer give rise to multiple quantum well like structure in which inorganic layer represents the potential well and insulating organic layer represents potential barrier.[2,7] So any charge carriers created in the semiconducting layer will not go into the insulating organic layer. So the charge carriers remain confined within the atomically thin inorganic layer, which is called as quantum confinement effect which is a well-known phenomenon observed in two dimensional hybrid organic-inorganic perovskites depicted in the figure 2 below in which E_g (well) represents the band gap corresponding to the inorganic layers.[2,7,17,23]

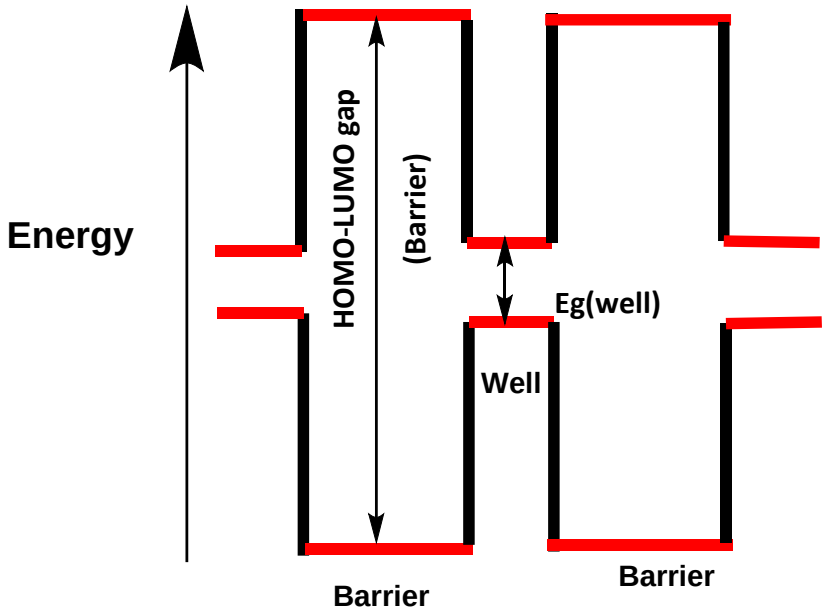

Figure 2: Multiple quantum well structure which enables the quantum confinement effect in 2D layered hybrid perovskites.

Also, the dielectric constant of the organic layer is very small compared to the inorganic layer. This give rise to high excitonic binding energy.[7] Excitonic binding energy is the measure of interaction between electron and hole held together by the coulombic interaction given by the formula, $F = Kq_1q_2/r^2$.Where q_1,q_2 are the charge of electron/hole, r is the distance between electron & hole in the excitonic state and $K = 1/4\pi\varepsilon$, ε is the dielectric constant of medium. This electron-hole pair is given by the name “exciton”. In case of 2D hybrid organic inorganic perovskite this excitonic binding energy is in the order of 300-400 meV compared to 3D perovskites which is around 20-50 meV.[22,23] Along with this, 2D perovskites show high moisture stability due to the bulkier organic ligands compared to the 3D perovskites.

On the other hand, doping metal ions into semiconductor hosts is a well known strategy to tailor optical, magnetic and electrical functionalities. Various transition metal ions doping in the perovskites has been reported which includes Mn^{2+}, Cd^{2+} and Zn^{2+} doping in $CsPbBr_3$.[3,4,25] Mn^{2+} in this 3D perovskites show a photoluminescence quantum yield of approx 30%.[2,4,25] Various studies on Mn^{2+} in both 3D as well as 2D perovskites have been reported showing a broad emission around 600 nm.[25] Rare earth ions have also been doped in case of 3D perovskites which includes Yb^{3+}, Er^{3+}, Tm^{3+} and Ce^{3+} among which Yb^{3+} emission around 990 nm could obtain a quantum efficiency more than 100% due to quantum cutting phenomena.[3,9,15] From our lab, Yb^{3+} doping in $CsPbX_3$ (X = Br, I) and $Cs_2AgInCl_6$ perovskite have been reported .[4,6,25] Doping of Yb^{3+} gives rise to new functionality like near infrared (NIR) emission which has its application in light emitting diodes (LEDs).[4,6,9,25] Lanthanide ion doping has advantage of negligible self-absorption hence it contributes to enhancement of its photoluminescence quantum yield and can emit pure NIR emission.[6,14]Among many of the available lanthanide ions, doping of Yb^{3+} is being exclusively studied, since it have simplest two energy states ($^2F_{7/2}$, $2F_{5/2}$) in excited state which helps to minimise the non radiative energy loss as compared to other lanthanide ions.[6,14,19] As per our knowledge, there is no report of lanthanide ion doping in 2D layered hybrid organic inorganic perovskites. This motivates us to dope Yb^{3+} in hybrid organic inorganic. In this thesis, we have doped Yb^{3+} into $(C_8H_9NH_3)_2PbBr_4$ nanoplatelets and have characterized the nanoplatelets and studied its NIR emission at 998 nm.

2 Methods

2.1 Chemicals:

Phenyl ethylamine (98%, Sigma-Aldrich), lead (II) acetate trihydrate (99.99%, Sigma-Aldrich), bromotrimethyl silane (TMSBr, 99%, Sigma-Aldrich), ytterbium (III) acetate tetra-hydrate (Yb $(C_2H_3O_2)_3.4H_2O$,99.9%, Sigma-Aldrich), ytterbium (III) nitrate penta-hydrate (Yb $(NO_3)_3.5H_2O$, 99.99%, Sigma-Aldrich), oleic acid (OA, 90%, Sigma-Aldrich), 1-octadecene (ODE, 90%, Sigma-Aldrich), Acetone (90%, FINAR), toluene (99.5%, Sigma-Aldrich). All chemicals were used without any further purification.

2.2 Synthesis of colloidal $(C_8H_9NH_3)_2PbBr_4$ nanoplatelets:

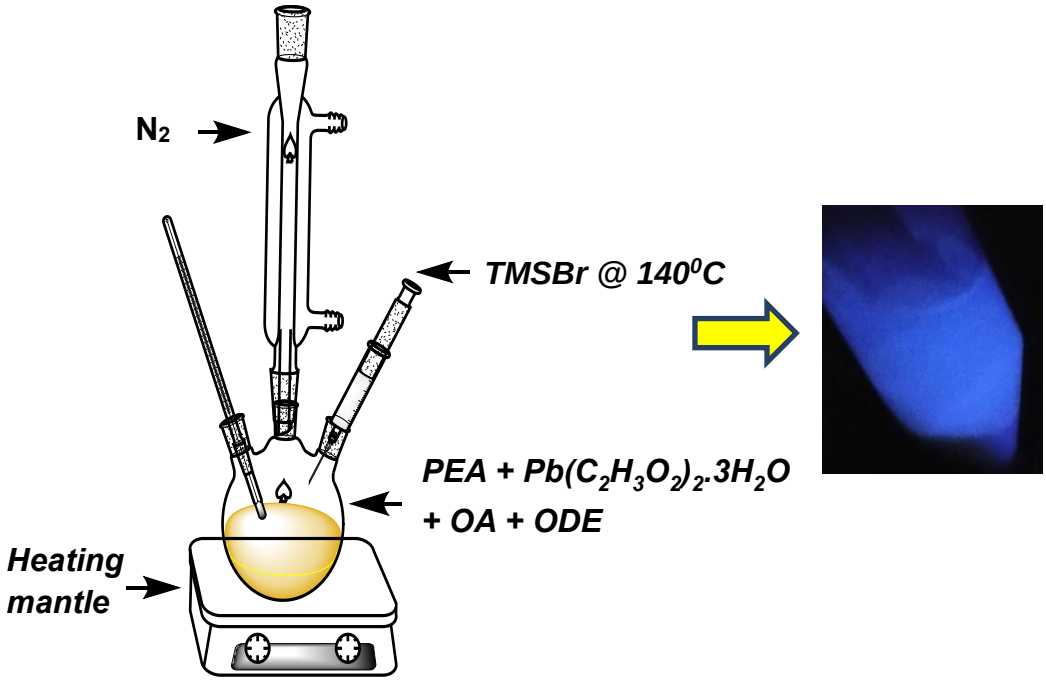

Figure 3: Schematic representation shows synthesis of colloidal $(C_8H_9NH_3)_2PbBr_4$ nanoplatelets using hot injection method showing bluish emission under UV light.

Synthesis of colloidal $(C_8H_9NH_3)_2PbBr_4$ nanoplatelets follows the hot injection method in which the halide precursor is injected in a solution containing other precursors at a particular temperature. Colloidal nanoplatelets were synthesized by using the hot injection method. In 3 necked round bottom flask, 1 ml OA, 10 ml ODE, 1.56 mmole of

PEA and 0.2 mmole lead acetate trihydrate were taken. N_2 gas were passed followed by application of vacuum (30 min each) to remove the moisture and dissolved oxygen. The reaction temperature was then set to 100 ˚C under constant stirring. The mixture color changed to pale yellow transparent solution after dissolution of all the precursors. Further, the temperature was set to 140 ˚C while under N_2 flow. After reaching this temperature, 0.2 ml TMSBr was quickly injected and the reaction by stopped after 5s and cooled using ice bath.

For the washing of the nanocrystals, the crude reaction product was first centrifuged at 7830 rpm for 10 minutes. To the precipitate 10 ml toluene was added and again centrifuged with the same rpm for 10 minute. The final precipitate was dispersed in 10 ml toluene and stored for further measurements.

2.3 Synthesis of Yb^{3+} doped 2D-$(C_8H_9NH_3)_2PbBr_4$ colloidal nanoplatelets

Colloidal Yb^{3+} doped $(C_8H_9NH_3)_2PbBr_4$ nanoplatelets were synthesized by the same hot injection method as discussed above except this time with the ytterbium precursors, such as ytterbium acetate tetrahydrate or ytterbium nitrate pentahydrate in required molar ratio.

2.4 Inductive coupled plasma atomic emission spectroscopy (ICP-AES)

ICP-AES was the technique used to determine the elemental composition in the Yb^{3+} doped $(C_8H_9NH_3)_2PbBr_4$ nanoplatelets products. It's an emission spectroscopy in which we use the inductive coupled plasma. This plasma is used to excite the atoms which will emit electromagnetic radiation when this excited sample relaxes to the lower energy states. The emitted radiation belongs to a particular wavelength which corresponds to a specific element which is collected by the detector. Normally the plasma which are used consist of high temperature high electron density argon gas. Based on the intensity of the emitted radiation wavelength and calibrated plot, concentration of element in the sample can be determined.

The samples are dissolved in 3:1 molar ratio of aquaregia. The concentration of samples kept ~10 ppm. In dopant element, ppm level is 100 ppm and normalised by

factor of 10. The ICP-AES measurements were carried out using using ARCOS simultaneous ICP spectrometer, SPECTRO Analytical Instruments GmbH, Germany

2.5 X-ray diffraction (XRD)

Powder XRD was used to analyse the crystal structure, and also to have qualitative idea about the size of crystals. Principle of the XRD is the constructive interference of the X ray beam with the periodically arranged particles in the crystal, which is nothing but the Bragg's condition

$$2d \sin\theta = n\lambda$$

where d is the inter-planar distance between two Bragg's planes in crystals, λ is the wavelength of the incident X-ray radiation and θ is the angle of diffraction. XRD patterns have been recorded using Bruker D8 Advance X-ray diffractometer with Cu Kα (1.54 Å) radiation. Samples for powder XRD measurements are prepared by drop casting concentrated colloidal dispersion on a glass slide.

2.6 Transmission electron microscopy (TEM)

To analyse the sample morphology in a detailed way TEM has been used. From high resolution TEM (HRTEM) we get information about the crystallinity of the sample. TEM images were recorded using a UHR FEG-TEM, JEOL JEM 2100F field emission transmission electron microscope at 200 kV. TEM samples are prepared by drop casting dilute dispersion of sample on a carbon coated Cu TEM grid.

2.7 Atomic force microscopy (AFM)

AFM gives the topographical images, thickness and height profiles of our sample. We have collected the images by using keysight atomic force microscope model AFM 5500 in the tapping mode. Samples were prepared by drop casting the diluted dispersion of $(C_8H_9NH_3)_2PbBr_4$ nanoplatelets which were dissolved in toluene on a silicon wafer and put it for drying for about 3 hours.

2.8 UV-Vis and UV-Vis-NIR absorption spectroscopy in transmission mode

In UV-Vis-NIR spectroscopy, when a beam of light passes through the sample, the light gets absorbed by the sample. The principle of UV-Vis and UV-Vis-NIR absorption spectroscopy follows the Beer-Lambert Law which is the linear relationship between absorbance and the concentration of a given sample.

$$A = \varepsilon.c.l$$

where A is the absorbance, C is the concentration and ε is the molar extinction coefficient of the material. UV-Vis absorption spectra of the colloidal nanocrystals were measured by Cary series spectrophotometers and UV-Vis-NIR absorption spectra by Shimadzu UV-3600 spectrophotometer.

2.9 UV-Vis-NIR diffused reflectance spectroscopy

In diffused reflectance spectroscopy, we measure the reflectance from the opaque sample surface. Significant amount of light gets scattered in all directions in case of solid sample while recording in reflectance mode. Such scattering is minimal for measurements of colloidal nameplates in the transmission. In diffused reflectance mode, the reflectance measured gets converted to absorbance by the Kubelka-Munk function

$$F(R) = (1-R)^2 / 2R = \alpha/S$$

R is the reflection, α is the absorbance coefficient and *S* is the scattering coefficient.[24]UV-Vis-NIR reflectance spectra were recorded by drop casting the sample on a glass slide in Shimadzu UV-3600 spectrophotometer.

2.10 Steady-state photoluminescence (PL) and PL decay dynamics

Samples are excited by steady state xenon lamp in steady state PL spectroscopy. For Yb^{3+} emission with ms scale lifetime, microsecond flash lamp was used. TCSPC (Time correlated single photon counting) was used for measuring PL decay dynamics.

Edinburg FLS 980 instrument was used for all the measurements including PL, PL excitation and PL decay dynamics.

2.11 Contact angle measurement

Contact angle measures the degree of wettability of a solid surface by the liquid. It helps to measure the hydrophobicity / hydrophilicity of a given material. We have carried out our measurements using Holmarc's contact angle meter. The nanoplatelets spin coated on a glass surface was used for the measurements.

3 Results and discussion

3.1 Structure and morphology of Yb^{3+} doped $(C_8H_9NH_3)_2PbBr_4$ nanoplatelets

We have synthesized 2D layered Yb^{3+} doped $(C_8H_9NH_3)_2PbBr_4$ nanoplatelets with varying concentration of Yb^{3+} ion including the undoped sample The nanoplatelets form colloidal dispersions in toluene. Toluene was chosen as the solvent because of its interaction with $C_8H_9NH_3^+$ in $(C_8H_9NH_3)_2PbBr_4$ nanoplatelets. The amine group of $C_8H_9NH_3^+$ is bonded to $\{PbBr_4\}^{2-}$ via hydrogen bonding whereas the hydrocarbon tail interacts with toluene, forming a colloidal dispersion of nanoplatelets in toluene.[13]

Table 1: Comparison of Yb^{3+} concentrations in the precursor as well as doping percentage obtained in the product

% Yb precursor taken	% Yb in product (ICP-AES)
33	3.4
50	2.4
66	27
71	48.6

From the ICP-AES we could clearly see that the doping percentage is not the same as that of the molar ratio of the Yb^{3+} precursor taken. ICP-AES was employed to obtain the Yb^{3+} concentration in all the product nanoplatelets with various precursor concentrations of Yb^{3+}. The final data with Yb^{3+} concentration is shown in table 1. Percentage concentration of Yb^{3+} is calculated by using the formula $\{[Yb]/([Yb]+[Pb])\} \times 100$. Yb^{3+} precursor concentrations vary from 33 to 71 % whereas the doping percentage in the product ranges from 3.4% to 48.6%. The doping percentages of 27% and 48.6% are unexpectedly high. We will require to do more measurements to check the reproducibility of these data. But based on this preliminary data, it appears that a small fraction of the Yb^{3+} ions probably gets into the lattice of nanoplatelets, and remaining amount of the dopants sticks to the surface or surroundings. Again we note that, reproducibility of this ICP-AES data wasn't done. Hence we will further reproduce this doping percentage in future. In any case, from here onwards, we mention the Yb^{3+} doping percentage obtained from the ICP-AES analysis in the rest of the thesis.

Figure 4 shows PXRD patterns of undoped as well as Yb^{3+} doped $(C_8H_9NH_3)_2PbBr_4$ nanoplatelets. The PXRD patterns shows peak at regular interval of two theta. This observation is characteristics of layered structure and each peak corresponding to its interlayer spacing.[2]Upon doping there is no change/shift in the PXRD peak positions. As interplanar distance (d) between the organic and inorganic layer is high it's expected to form 2D layered structure. Since the peak corresponding to interlayer spacing these are not expected to change while doping.

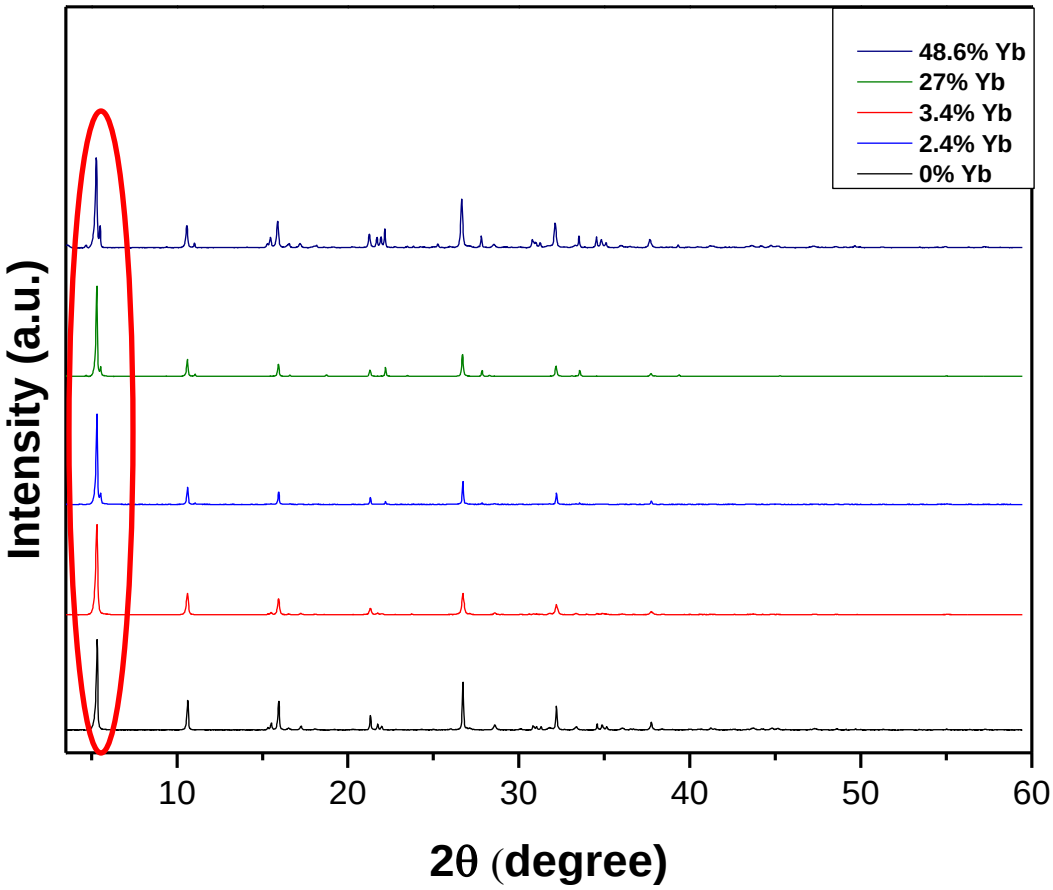

Figure 4: Powder XRD Patterns of Yb^{3+} doped as well as undoped $(C_8H_9NH_3)_2PbBr_4$

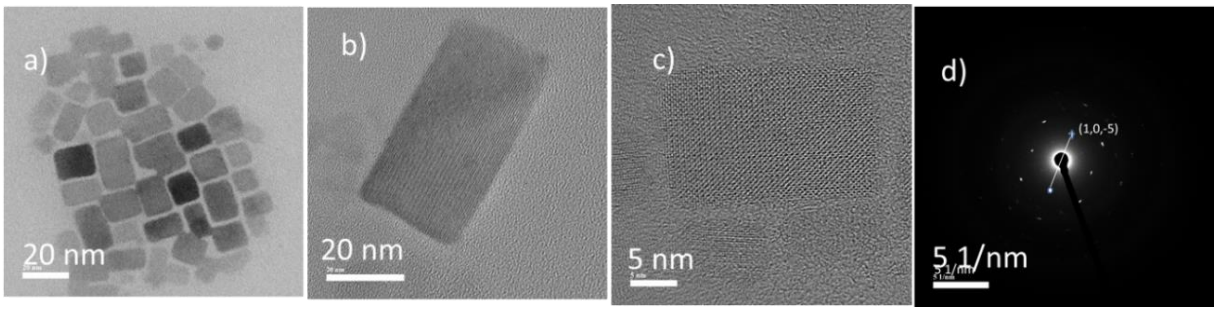

Figure 5: TEM images of a) $(C_8H_9NH_3)_2PbBr_4$ nanoplatelets; b) 2.4%Yb^{3+} doped $(C_8H_9NH_3)_2PbBr_4$ nanoplatelet. C) HRTEM Image of $(C_8H_9NH_3)_2PbBr_4$ nanoplatelet and d) SAED pattern of $(C_8H_9NH_3)_2PbBr_4$ nanoplatelet.

TEM and AFM images have been taken to study the morphology of the product. Figure 5 a represents the TEM image of $(C_8H_9NH_3)_2PbBr_4$ nanoplatelets. The lateral dimension of the undoped nanoplatelets is found to be 17 × 9 nm. Figure 5b represents the TEM image of the 2.4 % Yb^{3+} doped $(C_8H_9NH_3)_2PbBr_4$ nanoplatelets. Lattice fringes are visible confirming the crystalline nature of the nanoplatelets. Figure 5c represents the HRTEM image of undoped nanoplatelets. Figure 5d represents the selected area electron diffraction (SAED) of the undoped $(C_8H_9NH_3)_2PbBr_4$ nanoplatelet. From the SAED Pattern as well as HRTEM image, we could clearly see the single crystalline nature of the sample.

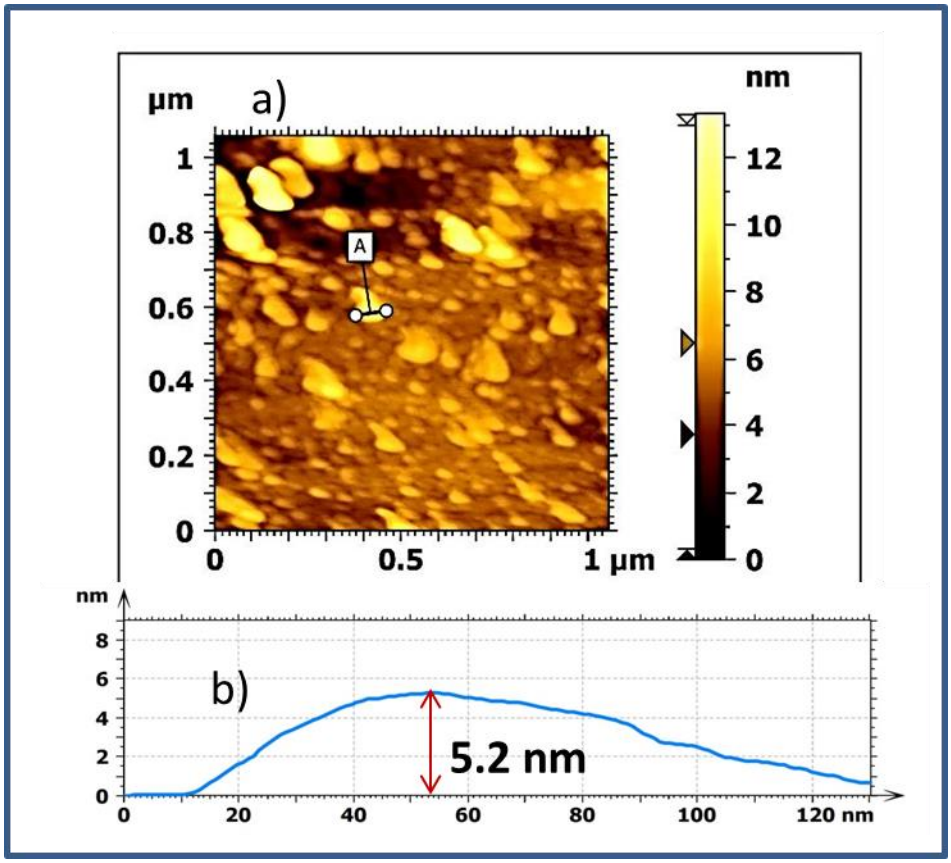

Figure 6 a) represent The AFM image of undoped $(C_8H_9NH_3)_2PbBr_4$ nanoplatelets and b) Corresponding height profile of the selected nanoplatelet shown by the line on AFM image.

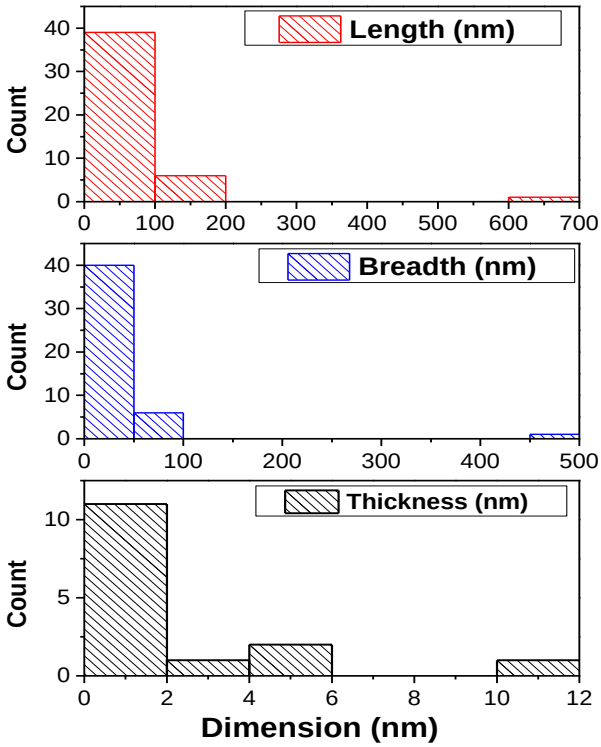

Figure 7: Size distribution histogram of $(C_8H_9NH_3)_2PbBr_4$ nanoplatelets showing dimension from AFM as well as TEM.

TEM images are projections of 3D objects onto a 2D screen. So, TEM images cannot measure the thicknesses (third dimension) of samples. To measure the thickness of our samples, we used AFM. Figure 6 represents the AFM images of undoped $(C_8H_9NH_3)_2PbBr_4$ nanoplatelet and its corresponding height profile. Figure 6 a) represent the AFM image of the $(C_8H_9NH_3)PbBr_4$ nanoplatelets. Figure b) Corresponding height profile of the selected nanoplatelet (130 nm dimension) shown by the line on AFM image. To check whether the third dimension (height) is of small (few 1-10 nm) order, we took the size distribution and measured the height corresponding to each nanoplatelets. After taking the size distribution, the data confirms that height ranges from 0.7 nm to 3 nm for approx. 100 nm width nanoplatelets. Height corresponds to the small dimension compared to its other dimension of a given sample, Hence from TEM as well as AFM we could confirm that it's a nanoplatelet. The size distribution plots which summarize the TEM and AFM data to conclude all the

dimension was given below in figure 7. Hence from TEM as well as AFM the dimension of $(C_8H_9NH_3)_2PbBr_4$ nanoplatelets are found to be 91 X 39.8 X 2.1nm.

3.2 Optical properties of of Yb^{3+} doped $(C_8H_9NH_3)_2PbBr_4$ nanoplatelets

After synthesis and characterization, we studied the optical properties of undoped and Yb^{3+} doped $(C_8H_9NH_3)_2PbBr_4$ nanoplatelets. Figure 8 a) represent the UV-Vis absorption spectra of 0%, 2.4%, 3.4%, 27% and 48.6% Yb^{3+} doped and undoped $(C_8H_9NH_3)_2PbBr_4$ nanoplatelets. The excitonic feature, which is the prominent feature of 2D perovskites can be visible at 406 nm (3.05 eV), which corresponds to the host absorption. The excitonic absorption peak position does not change upon Yb^{3+} doping. To check if there are any absorbance corresponds to Yb^{3+} in the NIR region, we measured UV-Vis-NIR absorption spectra of Yb^{3+} doped $(C_8H_9NH_3)_2PbBr_4$ nanoplatelets. There is no absorption feature in the NIR region corresponding to Yb^{3+} f-f electronic transitions.

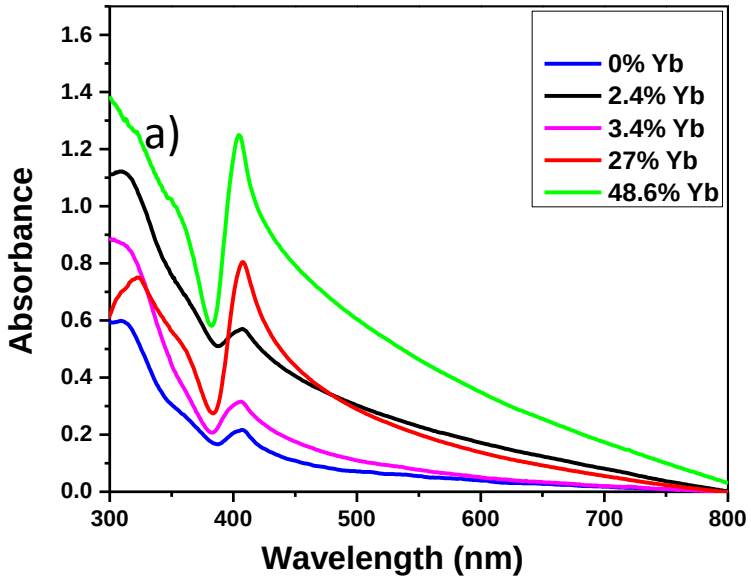

Figure 8: a) UV-Vis absorption spectra of undoped and Yb^{3+} doped $(C_8H_9NH_3)_2PbBr_4$ nanoplatelets.

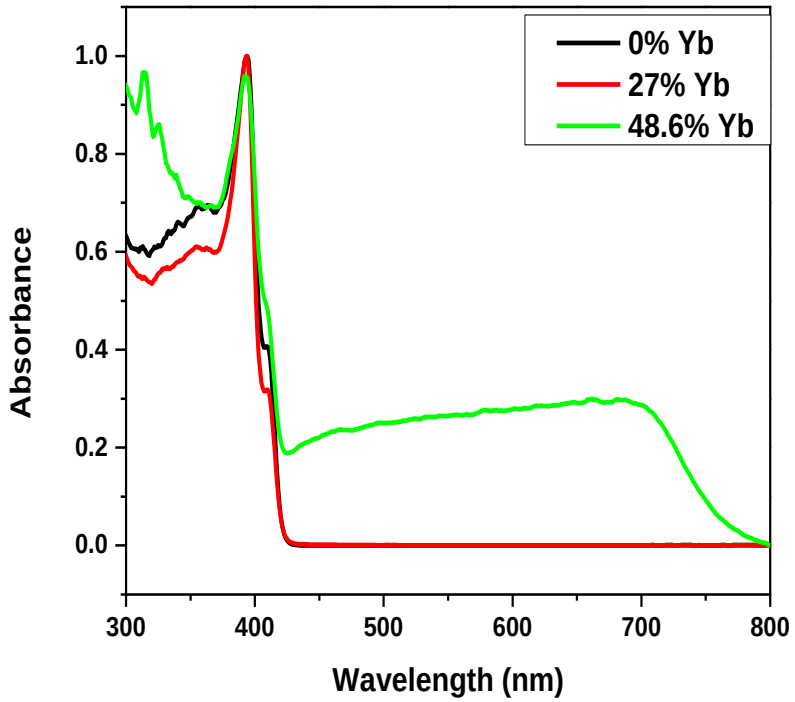

Figure 9: Diffused reflectance spectra of undoped and Yb^{3+} doped $(C_8H_9NH_3)_2PbBr_4$

Absorption spectra of colloidal dispersions shows tail towards longer wavelength end. To verify, whether the tail arises from sub-bandgap absorption or scattering of light by samples, we have measured diffused reflectance spectra (DRS) on the films of nanoplatelets. Figure 9 shows the diffused reflectance spectra (DRS) of undoped and Yb^{3+} doped $(C_8H_9NH_3)_2PbBr_4$ nanoplatelets. The undoped and 27% Yb^{3+} doped nanoplatelets do not show significant absorbance towards the longer wavelength in the DRS spectra. This observation suggests that the absorption tail observed for colloidal NCs in Figure 8 is due to scattering of light by the samples. In the DRS data (Figure 9) of 48.6% Yb^{3+} doped sample, we see an absorption feature at ~700 nm. This needs to be further verified.

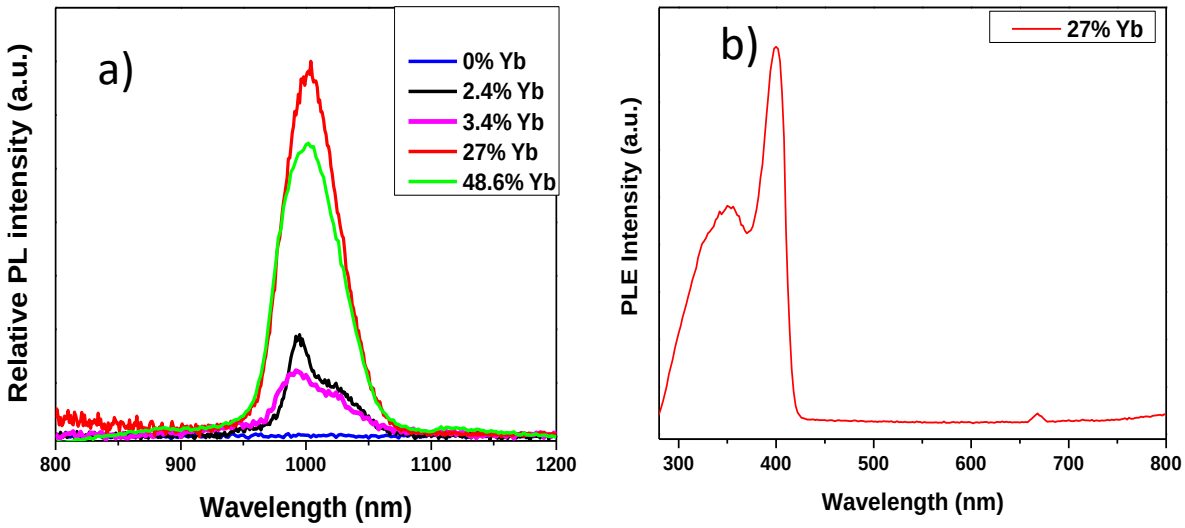

Figure 10 a) PL Spectra of undoped and Yb^{3+} doped $(C_8H_9NH_3)_2PbBr_4$ nanoplatelets showing Yb^{3+} emission in NIR region. b) PL excitation spectrum of Yb^{3+} emission (998 nm) in 27% Yb doped $(C_8H_9NH_3)_2PbBr_4$ nanoplatelets

Figure 10a represents the PL Spectra of 0%, 2.4%, 3.4%, 27% and 48.6% Yb^{3+} doped $(C_8H_9NH_3)_2PbBr_4$ nanoplatelets. An emission near 998 nm corresponds to Yb^{3+} emission could be seen in the PL emission spectra. The PL emission intensity increases with dopant concentrations and reaches to a maximum for 27% doping. Further increase in doping concentration to 48.6% decreases the PL intensity. Even though we are seeing the emission in the NIR region, in the UV-Vis-NIR absorption spectra there is no absorbance in the NIR region corresponding to this emission. This indicates that Yb^{3+} emission at 998 nm (1.24 eV) probably originated from the excitation of the host. To study this aspect, we have measured the PL excitation (PLE) spectrum of Yb^{3+} doped $(C_8H_9NH_3)_2PbBr_4$ nanoplatelets. Figure 10b shows PLE spectrum of 27% Yb^{3+} doped $(C_8H_9NH_3)_2PbBr_4$ nanoplatelets, fixing the emission wavelength at 998 nm. A PLE peak around 407 nm is observed. This PLE peak matches with the excitonic absorption of the host shown in Figure 8. These results show that hosts first get excited by absorbing light. Then the excitation energy is nonradiatively transferred to the Yb^{3+}

dopants exciting their f-electrons. Subsequent de-excitation of Yb^{3+} f-electrons gives rise to 998 nm emission.

Figure 11a represents the excitonic PL spectra of undoped as well as Yb^{3+} doped $(C_8H_9NH_3)_2PBr_4$ nanoplatelets. The excitonic emission of the host has peak at 415 nm. The intensity of excitonic emission decreases with increase in Yb^{3+} doping percentages. This decrease also supports the proposed energy transfer from host to the dopants. Also, note that there is no significant emission feature in the 460 nm which corresponds to Yb^{2+} emission.[8] Hence the observation of strong Yb^{3+} emission at 998 nm, and absence of Yb^{2+} emission suggest that the product nanoplatelets largely contain Yb^{3+} ions.

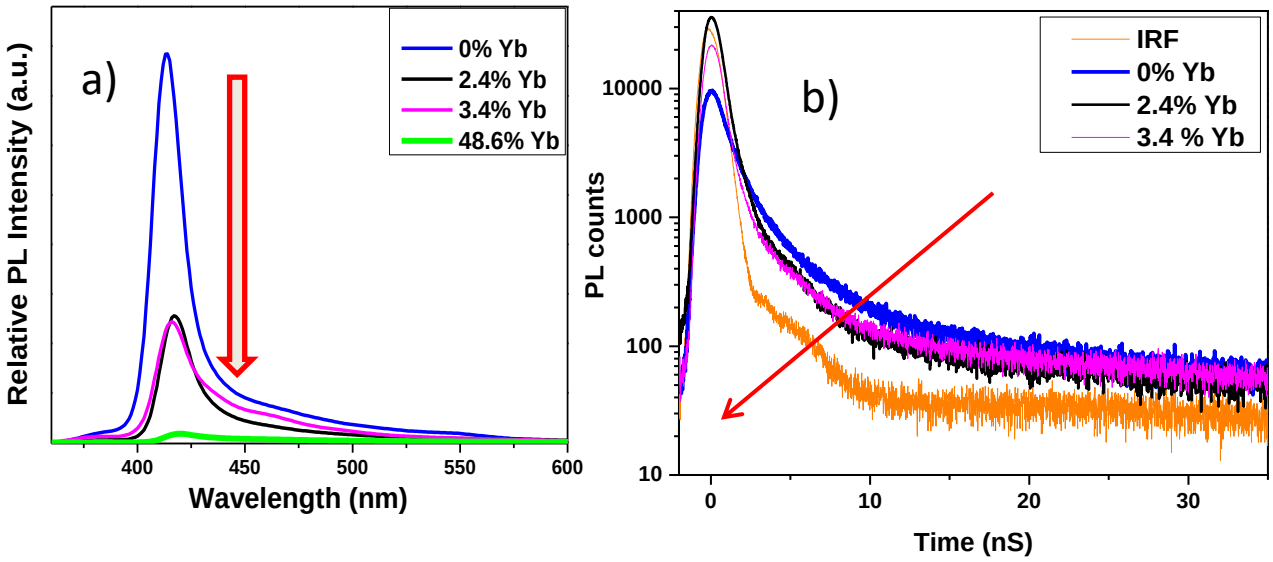

Figure 11: a) PL spectra of undoped and Yb^{3+} doped $(C_8H_9NH_3)_2PbBr_4$ nanoplatelets showing excitonic emission. b) PL decay dynamics of the excitonic emission at 415 nm Yb^{3+} doped $(C_8H_9NH_3)_2PbBr_4$ nanoplatelets with different doping percentage

Figure 11b represents the PL decay dynamics of host emission (415 nm) of Yb^{3+} doped $(C_8H_9NH_3)_2PbBr_4$ for different doping concentrations. PL decay becomes faster with an increase in Yb^{3+} concentration. This observation again supports faster non-radiative energy transfer from host to dopants. An increase in dopant concentration increases the faster non-radiative energy transfer, thereby decreasing the excitonic PL lifetime.

Therefore, PLE spectrum, along with decrease in both intensity and lifetime of excitonic PL together confirm that the Yb^{3+} emission originate via non-radiative excitation of the dopants by the $(C_8H_9NH_3)_2PbBr_4$ nanoplatelets hosts.

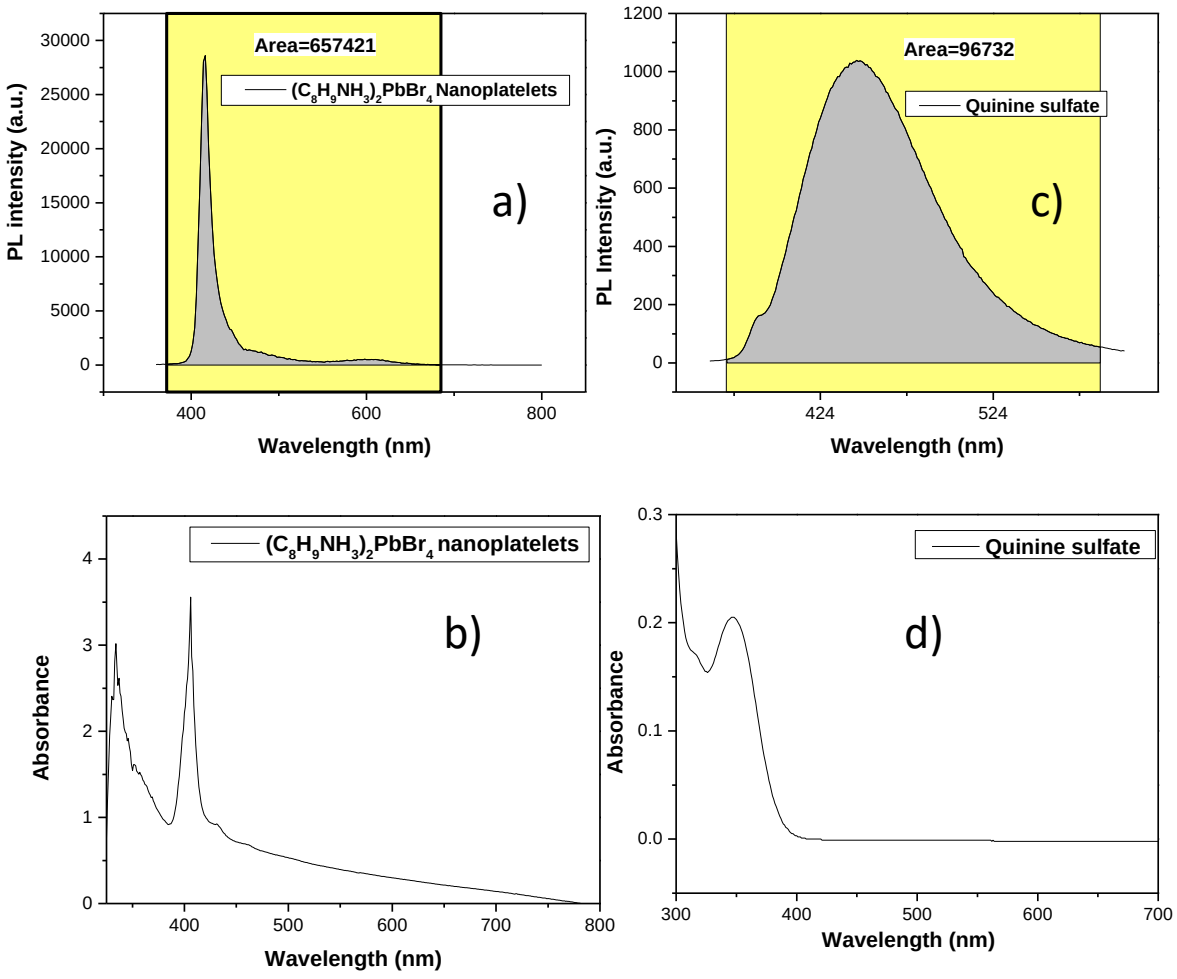

Figure 12: Estimation of PL quantum yield of excitonic emission of undoped $(C_8H_9NH_3)_2PbBr_4$ nanoplatelets with reference to quinine sulfate dye. PL and absorption data of the sample (a-b) and dye (c-d).

3.3 Photoluminescence quantum yield of $(C_8H_9NH_3)_2PbBr_4$ nanoplatelets

PL quantum yield is the measure of number of photons emitted / number of photons absorbed. PL quantum yield of colloidal $(C_8H_9NH_3)_2PbBr_4$ nanoplatelets was measured by taking a reference standard of quinine sulfate dye. The dye solution was prepared in 0.5 M HCl. The PLQY of sample is calculated by the formula,

$$PLQY(Sample) = PLQY(dye) * [I_{sample} * Adye(\lambda_{exc}) * (n^2_{sample}) / (I_{dye} * A_{sample}(\lambda_{exc}) * (n^2_{dye})]$$

Where,

I_{sample}= The integrated fluorescence of sample

I_{dye} = The integrated fluorescence of dye.

$Adye(\lambda_{exc})$ = Absorbance of dye at the excitation wavelength of PL

$A_{sample}(\lambda_{exc})$ = Absorbance of sample at the excitation wavelength of PL

n_{sample},= Refractive index of sample

n_{dye} = Refractive index of dye.

From figure 12, Integrated fluorescence intensity of the sample = 657421 and integrated fluorescence intensity of dye = 96732. Both sample and dye were excited at 340 nm.

Calculated PLQY= $0.546 * [(657421 * (0.195) * (1.49)^2) / (96732 * 2.23 * (1.33)^2)]$

= 40.7%

3.4 Contact angle measurements

We also measure contact angles of water drops on spin coated nanoplatelet films on glass substrate. Figure 13 represents the contact angle of water in undoped as well as 48.6% Yb^{3+} doped nanoplatelets. Contact angle of water for undoped sample is 129^o and that for 48.6% Yb^{3+} doped sample is 33^o. Since the angle is more than 90^o for the undoped sample, we can term it as hydrophobic. This hydrophobic nature is expected, which provides better moisture stability to this layered hybrid perovskites. Surprisingly the 48.6% Yb^{3+} sample show hydrophilic nature. This may be because of impurities in

the forms Yb^{3+} complexes, at higher precursor concentrations of Yb^{3+}. This aspect needs to be studied further.

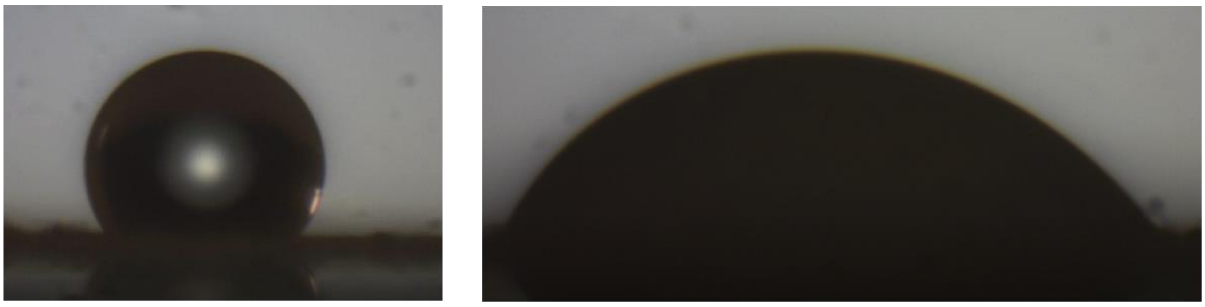

Figure 13: Contact angle measurement of water drops on films of a) undoped and b) 48.6% Yb^{3+} doped $(C_8H_9NH_3)_2PbBr_4$ nanoplatelets.

4 Conclusions

We have synthesised the colloidal Yb^{3+} doped $(C_8H_9NH_3)_2PbBr_4$ nanoplatelets. The colloidal stability is obtained for ~2 months. The nanoplatelets show a lateral dimension of 90.8 X 39.8 X 2.2 nm. From preliminary ICP-AES analysis we could see a small percentage of dopant is there in the product compared to the precursor concentration in the reaction mixture. The Yb^{3+} doped $(C_8H_9NH_3)_2PbBr_4$ nanoplatelets show NIR emission near 998 nm (1.24 eV). This new emission arise from f-f electronic transition of Yb^{3+} dopants. The intensity of Yb^{3+} emission increases with increasing dopant concentrations and reaches to a maximum (saturation point), after which a further increase in dopant concentration decreases the emission intensity. On the other hand the excitonic emission of undoped samples is intense with PLQY ~41%. Increasing the dopant concentration decreases the intensity of excitonic emission. To obtained mechanistic insights, we measured the PL excitation and PL decay dynamics. PLE shows that the 998 nm Yb^{3+} emission originate through the excitonic absorption of the host. PL decay dynamics also suggest the excitonic emission decays faster in the absence of Yb^{3+} dopants, suggesting a non-radiative energy transfer from the host to the dopant. All these results suggest the NIR emission is sensitized by the nanoplatelet

hosts. Lanthanide doping in 2D perovskite is a new topic, and to the best of our knowledge this is the first report of Yb^{3+} doping in 2D layered hybrid perovskites. Further study of these materials is expected to lead to applications in the field of NIR LEDs and remote sensing.

5. References

1. Ma, D.; Fu, Y.; Dang, L.; Zhai J.; Guzei, I.A.; Jin, S., Single-crystal microplates of two-dimensional organic–inorganic lead halide layered perovskites for optoelectronics. *Nano Res.* **2017**, 10, 2117–2129.

2. Sheikh, T.; Nag A., Mn doping in Centimetre sized Layered 2D Butyl ammonium lead bromide (BA_2PbBr_4) single crystal and their properties. *J. Phys. Chem. C.* **2019**, 123, 9420−9427.

3. Zhou, Y.; Chen, J.; Bakr, O.M.; Sun, H., Metal-doped lead halide perovskites: Synthesis, properties and opto electronic applications. *Chem. Mater.* **2018***,* 30, 6589−6613.

4. Mir, W.J.; Jagadeeswararao, M.; Das S.; Nag, A., Colloidal Mn doped Cs lead halide perovskite nanoplatelets. *ACS Energy Lett*. **2017**, 2, 537-543.

5. Liu, Y.; Yang, P., Self-Assembly of Two-Dimensional Perovskite Nano sheet Building

Blocks into Ordered Ruddelson−Popper Perovskite Phase. *J. Am. Chem. Soc.* **2019**, 141, 13028−13032.

6. Mahor, Y.; Mir, W. J.; Nag A., Synthesis and Near-Infrared Emission of Yb-Doped $Cs_2AgInCl_6$ Double Perovskite Microcrystals and Nanocrystals. *J. Phys. Chem. C* **2019***,* 123, 15787−15793.

7. Traore, B.; Pedesseau, L.; Assam, L.; Che X.; Blancon, J.C.; Tsai, H.; Nie, W.; Stoumpos, C. C.; Kanatzidis, M. G.; Tretiak, S. et al., Composite Nature of Layered

Hybrid Perovskites: Assessment on Quantum and Dielectric Confinements and Band Alignment. *ACS Nano* **2018***,* 12, 3321−3332.

8. Suta, M.; Urland, W.; Daul, C.; Wickleder, C., Photoluminescence properties of Yb^{2+} ions doped in the perovskites $CsCaX_3$ and $CsSrX_3$ (X = Cl, Br, and I) – a comparative study. *Phys. Chem. Chem. Phys*. **2016**, 18, 13196.

9. Crane, M. J.; Kroupa, D. M.; Gamelin, D. R., Detailed-balance analysis of Yb^{3+}:$CsPb(Cl_{1-x}Br_x)_3$ quantum-cutting layers for high-efficiency photovoltaics under real-world conditions. *Energy Environ. Sci.* **2019**, 12, 2486.

10. Dou, L.; Wong, A. B.; Yu, Y.; Lai, M.; Kornienko, N.; Eaton, S.W.; Fu, A.; Bischak, C. G.; Ma, J.; Ding, T. et al., Atomically thin two-dimensional organic-inorganic hybrid perovskites. *Science* **2015**, 349, 1518-1521.

11. Donega, C. M.; Liljeroth, P.; Vanmaekelbergh, D., Physicochemical Evaluation of the Hot-Injection Method, a Synthesis Route for Monodisperse Nanocrystal. *Small* **2005**, 1, 1152 – 1162

12. Shamsi, J.; Dang, Z.; Bianchini, P.; Canale, C.; Stasio, F. D.; Brescia, R.; Prato, M.; Manna, L., Colloidal synthesis of quantum confined single crystal $CsPbBr_3$ nanosheets with lateral size control up to the micrometer range. *J. Am. Chem. Soc*. **2016**, 138, 7240−7243.

13. Yang, S.; Niu, W.; Wang, A. L.; Fan, Z.; Chen, B.; Tan, C.; Lu, Q.; Zhang, H., Ultrathin Two-Dimensional Organic–Inorganic Hybrid Perovskite Nanosheets with Bright, Tunable Photoluminescence and High Stability. *Angew. Chem. Int. Ed*. **2017**, 56, 4252 –4255.

14. Milstein, T. J.; Kroupa, D. M.; Gamelin, D. R., Picosecond Quantum Cutting Generates Photoluminescence Quantum Yields Over 100% in Ytterbium-Doped $CsPbCl_3$ Nanocrystals. *Nano Lett*. 2018, 18, 3792-3799.

15. Zhou, D.; Liu, D.; Pan, G.; Chen, X.; Li, D.; Xu, W.; Bai, X.; Song H., Cerium and Ytterbium Codoped Halide Perovskite Quantum Dots: A Novel and Efficient

Downconverter for Improving the Performance of Silicon Solar Cells. *Adv. Mater.* **2017**, *29*, 1704149.

16. Mir, W. J. ; Sheikh, T.; Arfin, H.; Xia, Z.; Nag, A., Lanthanide doping in metal halide perovskite nanocrystals: spectral shifting, quantum cutting and optoelectronic applications. *NPG Asia Mater.* **2020**, 12, 9.

17. Tyagi, P.; Arveson, S. M.; Tisdale, W. A., Colloidal Organohalide Perovskite Nanoplatelets Exhibiting Quantum Confinement. *J. Phys. Chem. Lett*. **2015**, 6, 1911−1916.

18. Sapori, D.; Kepenekian, M.; Pedesseau, L.; Katan, C.; Even, J., Quantum confinement and dielectric profiles of colloidal nanoplatelets of halide inorganic and hybrid organic-inorganic perovskites. *Nanoscale*. **2016**, 8, 6369-6378.

19. Zhang, X.; Zhang, Y.; Zhang, X.; Yin, W.; Wang, Y.; Wang, H.; Lu, M.; Li, Z.; Gu, Z.; Yu, W. W., Yb^{3+} and Yb^{3+}/Er^{3+} doping for near-infrared emission and improved stability of $CsPbCl_3$ nanocrystals*. J. Mater. Chem. C*, 2018, **6**, 10101-10105.

20. Saparov, B.; Mitzi, D. B., Organic−Inorganic Perovskites: Structural Versatility for Functional Materials Design. *Chem. Rev*. **2016**, 116, 4558−4596.

21 Pan, G.; Bai, X.; Yang, D.; Chen, X.; Jing, P.; Qu, S.; Zhang, L.; Zhou, D.; Zhu, J.; Xu, W. et al., Doping lanthanide into perovskite nanocrystals: highly improved and expanded optical properties. *Nano Lett*. **2017**, 17, 8005−8011.

22. Tanaka, K.; Takahashi, T.; Kondo, T.; Umebayashi, T.; Asai, K.; Ema, K. Image Charge Effect on Two-Dimensional Excitons in an Inorganic-Organic Quantum-well Crystal. *Phys. Rev. B*. **2005**, 71, 045312.

23. Takagi, H.; Kunugita, H.; Ema, K., Influence of the Image Charge Effect on Excitonic Energy Structure in Organic-Inorganic Multiple Quantum Well Crystals. *Phys. Rev. B.* **2013**, 87, 125421.

24. Eickhoff, T.; Grosse, P.; Theiss, W., Diffuse Reflectance Spectroscopy of Powders. *Vib. Spectrosc.* **1990**, *1*, 229-233.

25.Mir W.J.; Mahor Y.; Lohar A.; Jagadeeswararao M.; Das S.; Mahumani S.; Nag A. Postsynthesis Mn and Yb doping into $CsPbX_3$ (X= Cl, Br, or I) provskite nanocrystals for downconversion emission. *Chem. Mater.* **2018**, 30, 22, 8170-8178

Copyright of ref.1

SPRINGER NATURE LICENSE
TERMS AND CONDITIONS

Mar 26, 2020

This Agreement between THEJASWI, PANUNDA, PO-ERUVATTY, PIN-670642, KANNUR, KERALA ("You") and Springer Nature ("Springer Nature") consists of your license details and the terms and conditions provided by Springer Nature and Copyright Clearance Center.

License Number	4790791357898
License date	Mar 16, 2020
Licensed Content Publisher	Springer Nature
Licensed Content Publication	Nano Research
Licensed Content Title	Single-crystal microplates of two-dimensional organic–inorganic lead halide layered perovskites for optoelectronics

Licensed Content Author	Dewei Ma et al
Licensed Content Date	Jan 18, 2017
Type of Use	Thesis/Dissertation
Requestor type	academic/university or research institute
Format	print
Portion	figures/tables/illustrations
Number of figures/tables/illustrations	1
Will you be translating?	no
Circulation/distribution	1 - 29
Author of this Springer Nature content	no
Title	Doping in lead halide perovskites

Institution name	Indian institute of science education and research
Expected presentation date	May 2020
Portions	Figure 1
	THEJASWI, PANUNDA, PO-ERUVATTY, PIN-670642, KANNUR, KERALA THEJASWI, PANUNDA, PO-ERUVATTY, PIN-6706
Requestor Location	THALASSERY, KERALA 670642 India Attn: THEJASWI, PANUNDA, PO-ERUVATTY, PIN-670642, KANNUR, KERALA
Total	0.00 USD

Terms and Conditions

Springer Nature Customer Service Centre GmbH
Terms and Conditions

This agreement sets out the terms and conditions of the licence (the **Licence**) between you and **Springer Nature Customer Service Centre GmbH** (the **Licensor**). By clicking 'accept' and completing the transaction for the material (**Licensed Material**), you also confirm your acceptance of these terms and conditions.

1. Grant of License

1. 1. The Licensor grants you a personal, non-exclusive, non-transferable, world-wide licence to reproduce the Licensed Material for the purpose specified in your order only. Licences are granted for the specific use requested in the order and for no other use, subject to the conditions below.

1. 2. The Licensor warrants that it has, to the best of its knowledge, the rights to license reuse of the Licensed Material. However, you should ensure that the material you are requesting is original to the Licensor and does not carry the copyright of another entity (as credited in the published version).

1. 3. If the credit line on any part of the material you have requested indicates that it was reprinted or adapted with permission from another source, then you should also seek permission from that source to reuse the material.

2. Scope of Licence

2. 1. You may only use the Licensed Content in the manner and to the extent permitted by these Ts&Cs and any applicable laws.

2. 2. A separate licence may be required for any additional use of the Licensed Material, e.g. where a licence has been purchased for print only use, separate permission must be obtained for electronic re-use. Similarly, a licence is only valid in the language selected and does not apply for editions in other languages unless additional translation rights have been granted separately in the licence. Any content owned by third parties are expressly excluded from the licence.

2. 3. Similarly, rights for additional components such as custom editions and derivatives require additional permission and may be subject to an additional fee. Please apply to Journalpermissions@springernature.com/bookpermissions@springernature.com for these rights.

2. 4. Where permission has been granted **free of charge** for material in print, permission may also be granted for any electronic version of that work, provided that the material is incidental to your work as a whole and that the electronic version is essentially equivalent to, or substitutes for, the print version.

2. 5. An alternative scope of licence may apply to signatories of the STM Permissions Guidelines, as amended from time to time.

3. Duration of Licence

3. 1. A licence for is valid from the date of purchase ('Licence Date') at the end of the relevant period in the below table:

Scope of Licence	Duration of Licence
Post on a website	12 months
Presentations	12 months
Books and journals	Lifetime of the edition in the language purchased

4. Acknowledgement

4. 1. The Licensor's permission must be acknowledged next to the Licenced Material in print. In electronic form, this acknowledgement must be visible at the same time as the figures/tables/illustrations or abstract, and must be hyperlinked to the journal/book's homepage. Our required acknowledgement format is in the Appendix below.

5. Restrictions on use

5. 1. Use of the Licensed Material may be permitted for incidental promotional use and

minor editing privileges e.g. minor adaptations of single figures, changes of format, colour and/or style where the adaptation is credited as set out in Appendix 1 below. Any other changes including but not limited to, cropping, adapting, omitting material that affect the meaning, intention or moral rights of the author are strictly prohibited.

5. 2. You must not use any Licensed Material as part of any design or trademark.

5. 3. Licensed Material may be used in Open Access Publications (OAP) before publication by Springer Nature, but any Licensed Material must be removed from OAP sites prior to final publication.

6. Ownership of Rights

6. 1. Licensed Material remains the property of either Licensor or the relevant third party and any rights not explicitly granted herein are expressly reserved.

7. Warranty

IN NO EVENT SHALL LICENSOR BE LIABLE TO YOU OR ANY OTHER PARTY OR ANY OTHER PERSON OR FOR ANY SPECIAL, CONSEQUENTIAL, INCIDENTAL OR INDIRECT DAMAGES, HOWEVER CAUSED, ARISING OUT OF OR IN CONNECTION WITH THE DOWNLOADING, VIEWING OR USE OF THE MATERIALS REGARDLESS OF THE FORM OF ACTION, WHETHER FOR BREACH OF CONTRACT, BREACH OF WARRANTY, TORT, NEGLIGENCE, INFRINGEMENT OR OTHERWISE (INCLUDING, WITHOUT LIMITATION, DAMAGES BASED ON LOSS OF PROFITS, DATA, FILES, USE, BUSINESS OPPORTUNITY OR CLAIMS OF THIRD PARTIES), AND
WHETHER OR NOT THE PARTY HAS BEEN ADVISED OF THE POSSIBILITY OF SUCH DAMAGES. THIS LIMITATION SHALL APPLY NOTWITHSTANDING ANY FAILURE OF ESSENTIAL PURPOSE OF ANY LIMITED REMEDY PROVIDED

8. Limitations

8. 1. ***BOOKS ONLY:*** Where **'reuse in a dissertation/thesis'** has been selected the following terms apply: Print rights of the final author's accepted manuscript (for clarity, NOT the published version) for up to 100 copies, electronic rights for use only on a personal website or institutional repository as defined by the Sherpa guideline (www.sherpa.ac.uk/romeo/).

9. Termination and Cancellation

9. 1. Licences will expire after the period shown in Clause 3 (above).

9. 2. Licensee reserves the right to terminate the Licence in the event that payment is not received in full or if there has been a breach of this agreement by you.

Appendix 1 — Acknowledgements:

For Journal Content:
Reprinted by permission from **[the Licensor]**: **[Journal Publisher** (e.g. Nature/Springer/Palgrave)] **[JOURNAL NAME] [REFERENCE CITATION** (Article name, Author(s) Name), **[COPYRIGHT]** (year of publication)

For **Advance Online Publication papers:**
Reprinted by permission from **[the Licensor]**: **[Journal Publisher** (e.g. Nature/Springer/Palgrave)] **[JOURNAL NAME] [REFERENCE CITATION** (Article name, Author(s) Name), **[COPYRIGHT]** (year of publication), advance online publication, day month year (doi: 10.1038/sj.[JOURNAL ACRONYM].)

For Adaptations/Translations:

For Adaptations/Translations:
Adapted/Translated by permission from **[the Licensor]**: **[Journal Publisher** (e.g. Nature/Springer/Palgrave)] **[JOURNAL NAME] [REFERENCE CITATION** (Article name, Author(s) Name), **[COPYRIGHT]** (year of publication)

Note: For any republication from the British Journal of Cancer, the following credit line style applies:

Reprinted/adapted/translated by permission from **[the Licensor]**: on behalf of Cancer Research UK: : **[Journal Publisher** (e.g. Nature/Springer/Palgrave)] **[JOURNAL NAME] [REFERENCE CITATION** (Article name, Author(s) Name), **[COPYRIGHT]** (year of publication)

For **Advance Online Publication** papers:
Reprinted by permission from The **[the Licensor]**: on behalf of Cancer Research UK: **[Journal Publisher** (e.g. Nature/Springer/Palgrave)] **[JOURNAL NAME] [REFERENCE CITATION** (Article name, Author(s) Name), **[COPYRIGHT]** (year of publication), advance online publication, day month year (doi: 10.1038/sj. [JOURNAL ACRONYM])

For Book content:
Reprinted/adapted by permission from **[the Licensor]**: **[Book Publisher** (e.g. Palgrave Macmillan, Springer etc) **[Book Title]** by **[Book author**(s)] **[COPYRIGHT]** (year of publication)

Other Conditions:

Version 1.2

Questions? customercare@copyright.com or +1-855-239-3415 (toll free in the US) or +1-978-646-2777.